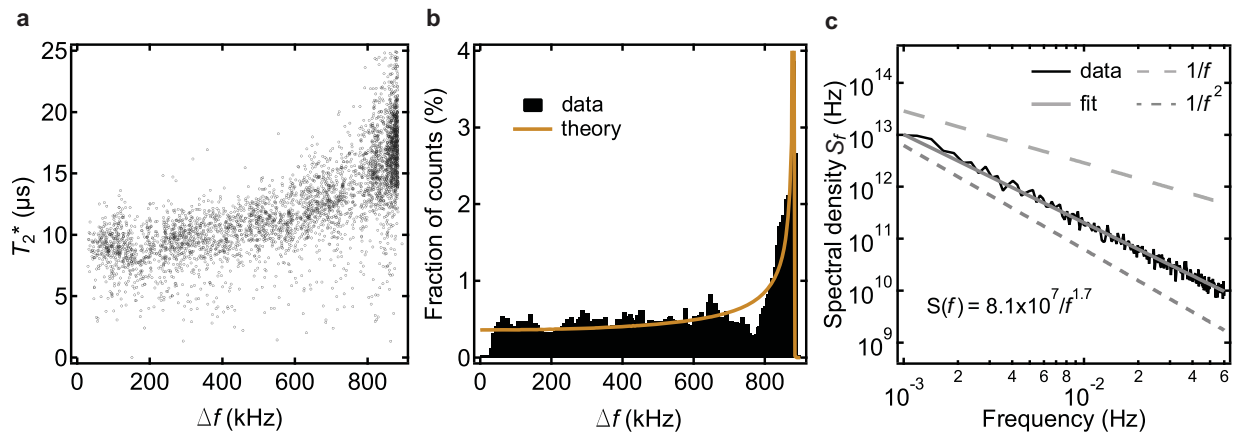


# Supplementary Information for “Millisecond charge-parity fluctuations and induced decoherence in a superconducting transmon qubit”

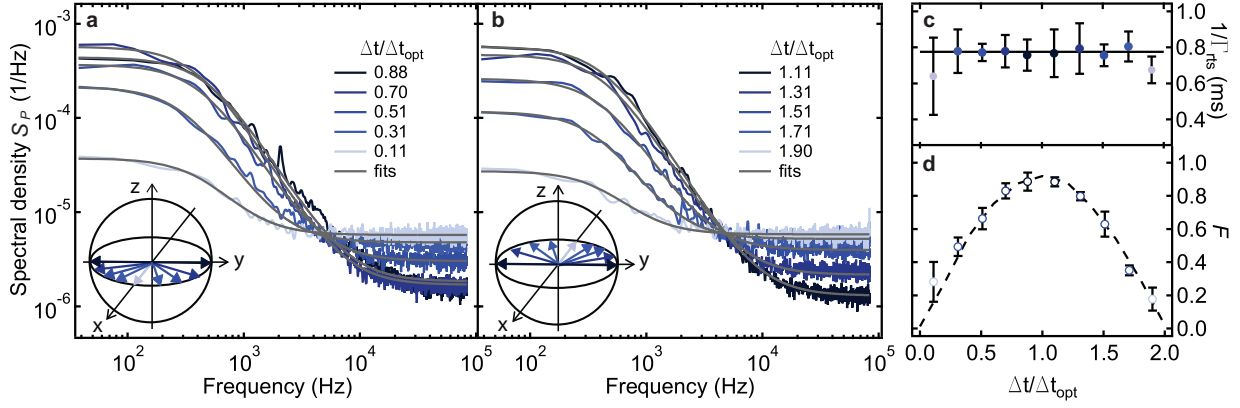
D. Ristè,<sup>1</sup> C. C. Bultink,<sup>1</sup> M. J. Tiggelman,<sup>1</sup> R. N. Schouten,<sup>1</sup> K. W. Lehnert,<sup>2</sup> and L. DiCarlo<sup>1</sup>

<sup>1</sup>*Kavli Institute of Nanoscience, Delft University of Technology,  
P.O. Box 5046, 2600 GA Delft, The Netherlands*

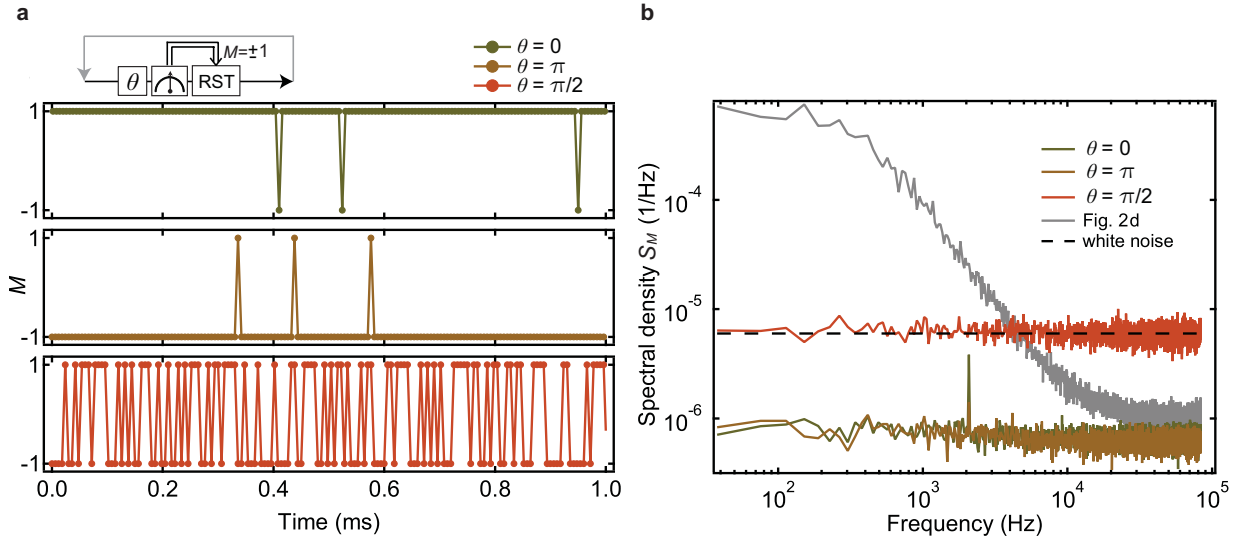
<sup>2</sup>*JILA, National Institute of Standards and Technology and Department of Physics,  
University of Colorado, Boulder, Colorado 80309, USA*



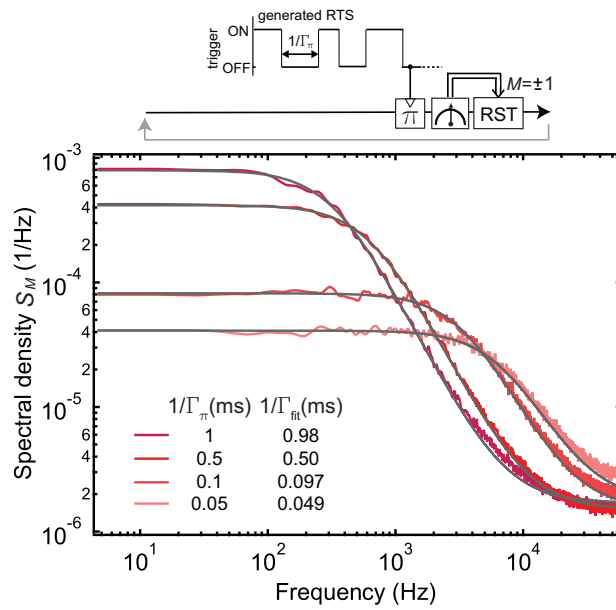
**Supplementary Fig. S1: qubit dephasing and charge noise.** **a**, Scatter plot of  $T_2^*$  as a function of  $\Delta f$  (see Fig. 1). The slow drift of the two frequencies evident in Fig. 1c is attributed to motion of background charges on the sapphire substrate, which capacitively couple to the qubit islands. In support of this hypothesis,  $T_2^*$  follows an upward trend with increasing  $\Delta f$ , with maximum ( $20 - 25 \mu\text{s}$ ) at the charge sweet spot ( $\Delta f_{\text{max}} = 880 \text{ kHz}$ ). **b**, Histograms of  $\Delta f$ , obtained from 30,000 Ramsey experiments acquired at  $\sim 4 \text{ s}$  interval, with 5 kHz binning. The distribution peaks at the charge sweet spot, where the qubit transition frequency is least sensitive to background charge fluctuations. The histograms are in good agreement with a sampled sinusoidal function, as expected for charge-modulated qubit frequency. **c**, Frequency power spectrum obtained from data in (b). We fit the equation  $A/f^\alpha$  to the data for  $f > 10^{-3} \text{ Hz}$ , giving best-fit values  $A = 8.1 \cdot 10^7$  and  $\alpha = 1.7$  (solid line). Dashed lines indicate the slopes for  $\alpha = 1, 2$ . The measured  $T_2^*$  is consistent in order of magnitude with that estimated from the frequency power spectrum.



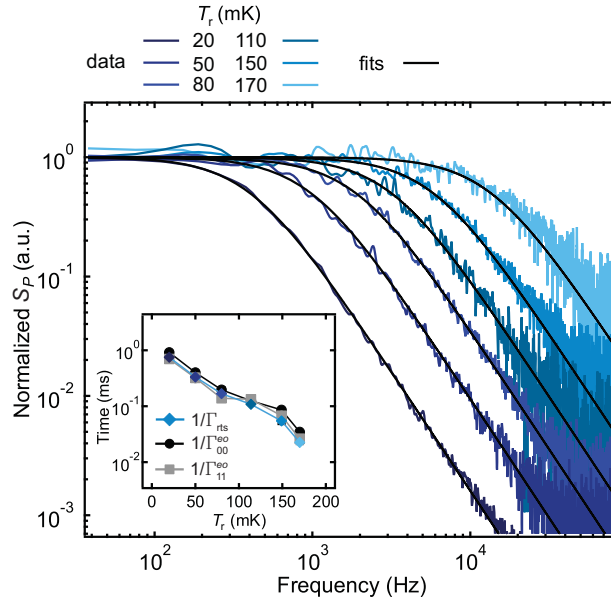
**Supplementary Fig. S2: Intentionally imperfect detector.** Power spectral densities similar to those in Fig. 2, but with Ramsey time  $\Delta t$  varied from the optimum  $\Delta t_{\text{opt}} = 1/4\Delta f$ . The detection fidelity  $F$  (d) decreases for **a**,  $\Delta t < \Delta t_{\text{opt}}$  and **b**,  $\Delta t > \Delta t_{\text{opt}}$  (b), but the extracted switching time  $1/\Gamma_{\text{rts}}$  remains approximately the same, as expected (c). Curves in c are obtained from a numerical simulation using  $1/\Gamma_{\text{rts}} = 0.78$  ms.



**Supplementary Fig. S3: Control experiment replacing the Ramsey sequence in Fig. 2 by a  $\theta$ -rotation of the qubit.** **a**, 1 ms snapshots of measurements taken at  $6 \mu\text{s}$  interval, over 48 ms. From top to bottom:  $\theta = 0, \pi$ , and  $\pi/2$ . For  $\theta = 0(\pi)$ ,  $M = 1(-1)$ , with  $\sim 1\%$  error, vastly improving on the fast reset demonstrated in Ref. 29. For  $\theta = \pi/2$ ,  $M$  is randomized by projection noise. **b**, Power spectral densities of **a**. For  $\theta = \pi/2$  the spectrum equals the white noise level (dashed line) at the sampling time of  $6 \mu\text{s}$ . For  $\theta = 0$  or  $\pi$ , the spectrum is an order of magnitude lower than the white noise level. The pickup at 2.1 kHz is associated with the pulse tube of the cryogen-free dilution refrigerator, as it disappears when the pulsed-tube compressor is momentarily turned off. The charge-parity spectrum from Fig. 2d is added for comparison.



**Supplementary Fig. S4: Power spectra of software-generated symmetric RTS, as detected by the qubit.** Programmed sequences of symmetric RTS with switching rate  $\Gamma_\pi$  are loaded into an ADwin controller that triggers a  $\pi$  pulse on the qubit when the level is high (similar to Ref. 25). The qubit is then measured and reset to  $|0\rangle$  every  $9 \mu\text{s}$ . This sequence emulates a RTS process similar to QP tunneling. The detected and programmed switching rates match to better than 3% over the range 0.05 to 1 ms.



**Supplementary Fig. S5: Charge-parity spectra at various refrigerator temperatures  $T_r$ .** Equation (1) in the main text is fit to each spectrum. To facilitate comparison, data and fits have the white noise offset subtracted and are renormalized. Inset: best-fit  $1/\Gamma_{\text{rts}}$  as a function of  $T_r$ .  $1/\Gamma_{00}^{e0}$  and  $1/\Gamma_{11}^{e0}$  (Fig. 4d) are also plotted for comparison.